JVI
Journals.ASM.org

Infectious Spleen and Kidney Necrosis Virus (a Fish Iridovirus) Enters Mandarin Fish Fry Cells via Caveola-Dependent Endocytosis

Chang-Jun Guo,[a,b] Yan-Yan Wu,[b] Li-Shi Yang,[b] Xiao-Bo Yang,[b] Jian He,[b] Shu Mi,[b] Kun-Tong Jia,[b] Shao-Ping Weng,[b] Xiao-Qiang Yu,[c] and Jian-Guo He[a,b]

MOE Key Laboratory of Aquatic Product Safety, School of Marine Science, Sun Yat-sen University, Guangzhou, People's Republic of China[a]; State Key Laboratory for Biocontrol, School of Life Sciences, Sun Yat-sen University, Guangzhou, People's Republic of China[b]; and Division of Cell Biology and Biophysics, School of Biological Sciences, University of Missouri—Kansas City, Kansas City, Missouri, USA[c]

Infectious spleen and kidney necrosis virus (ISKNV) is the type species of the genus *Megalocytivirus* from the family *Iridoviridae*. Megalocytiviruses have been implicated in more than 50 fish species infections and currently threaten the aquaculture industry, causing great economic losses in China, Japan, and Southeast Asia. However, the cellular entry mechanisms of megalocytiviruses remain largely uncharacterized. In this study, the main internalization mechanism of ISKNV was investigated by using mandarin fish fry (MFF-1) cells. The progression of ISKNV infection is slow, and infection is not inhibited when the cells are treated with ammonium chloride (NH_4Cl), chloroquine, sucrose, and chlorpromazine, which are inhibitors of clathrin-dependent endocytosis. The depletion of cellular cholesterol by methyl-β-cyclodextrin results in the significant inhibition of ISKNV infection; however, the infection is resumed with cholesterol replenishment. Inhibitors of caveolin-1-involved signaling events, including phorbol 12-myristate 13-acetate (PMA), genistein, and wortmannin, impair ISKNV entry into MFF-1 cells. Moreover, ISKNV entry is dependent on dynamin and the microtubule cytoskeleton. Cofraction analysis of ISKNV and caveolin-1 showed that ISKNV colocates with caveolin-1 during virus infection. These results indicate that ISKNV entry into MFF-1 cells proceeds via classical caveola-mediated endocytosis and is dependent on the microtubules that serve as tracks along which motile cavicles may move via a caveola-caveosome-endoplasmic reticulum (ER) pathway. As a fish iridovirus, ISKNV entry into MFF-1 cells is different from the clathrin-mediated endocytosis of frog virus 3 entry into mammalian cells (BHK-21) at 28°C, which has been recognized as a model for iridoviruses. Thus, our work may help further the understanding of the initial steps of iridovirus infection.

The essential events involved in a successful viral infection cycle include the specific attachment of a viral structural protein to a cellular receptor, followed by the internalization of the virus into the host cells and the subsequent uncoating of the virion to release viral genomes (51). For efficient cell entry, many animal viruses employ several different endocytosis pathways. Of these pathways, two have been proven to be the most frequently used: the clathrin-dependent entry pathway and the caveola-mediated endocytosis pathway (48).

Clathrin-mediated endocytosis is the best-characterized pathway and is considered the primary route of endocytosis entry into cells. A large number of viruses that enter host cells through a clathrin-mediated pathway (CMP) have been identified, such as Semliki Forest virus (SFV) (50), the polyomavirus JC virus (JCV) (44), influenza virus (6), West Nile virus (10), African swine fever virus (24), hantaan virus (26), dengue virus serotype 2 (43), and rubella virus (27), among others. This type of endocytosis involves clathrin-coated pit (CCP) formation, assembly, and budding, followed by CCP transport into acidic endosomal and lysosomal compartments and the *trans*-Golgi network (39). The prevention of the assembly of CCPs at the plasma membrane by hypertonic sucrose or chlorpromazine could inhibit the clathrin-mediated uptake of viruses (34). In the endosomes and lysosomes, a low pH triggers penetration; thus, the clathrin-mediated endocytosis pathway is sensitive to changes in pH in these low-pH compartments by reagents, such as chloroquine (CQ) and ammonium chloride (NH_4Cl), resulting in an inhibition of viral infection (13).

An alternative to the clathrin-mediated pathway, endocytosis via caveolae, is another well-characterized pathway. The first knowledge of this pathway was based mainly on the entry mechanism of simian virus 40 (SV40) (1). In this mechanism, viruses bind to a specialized membrane domain composed of sphingolipids and cholesterol, called caveolae. Morphologically, caveolae are 50- to 100-nm flask-shaped plasma membrane invaginations present in most cell types (17). The formation of caveolae is mediated by the marker protein caveolin-1. Caveolin-1 plays an important role in the stabilization of the plasma membrane association of caveolae, rather than the induction of raft invagination (35). Frequently, caveolae on most cell surface have little motility and dynamics. However, a signal cascade caused by the activation of tyrosine kinases could result in slow but efficient internalization (30). Accumulating evidence shows that endocytosis mediated by caveolae requires unique structural and signaling machinery (caveolin-1 and Src kinase), indicating that caveolar endocytosis occurs through a mechanism that is distinct from those of other forms of lipid microdomain associations and signaling event-dependent endocytosis (7). Ligands internalized via caveolae will later be delivered to several different compartments. For instance, SV40 and cholera toxin (CTx) are delivered to caveolin-1-

Received 30 November 2011 **Accepted** 1 December 2011
Published ahead of print 14 December 2011
Address correspondence to Jian-Guo He, lsshjg@mail.sysu.edu.cn.
C.-J. Guo and Y.-Y. Wu contributed equally to this work.

doi:10.1128/JVI.06947-11

positive, pH-neutral endocytosis compartments distinct from the compartments of the classical endocytosis and exocytosis pathways, the so-called caveosome, and then transported to the Golgi complex and the endoplasmic reticulum (ER), respectively (41). As for the others, such as the autocrine motility factor (AMF), they are delivered directly to the Golgi complex (31). Considering all the characteristics of caveolae mentioned above, internalization into the host cells via caveolae is a clathrin-independent pathway, which is sensitive to cholesterol depletion, associated with signaling events, and dynamin dependent (35). Since its discovery, the use of caveolae for entry into host cells has been demonstrated for other viruses, such as amphotropic murine leukemia virus (2), enteroviruses (33), coronavirus 229E (37), and foot-and-mouth disease virus (3), among others.

Iridoviruses are large icosahedral cytoplasmic DNA viruses that contain circularly permutated, terminally redundant, double-stranded DNA genomes (20). The current members of the family *Iridoviridae* are divided into five genera: *Iridovirus*, *Chloriridovirus*, *Ranavirus*, *Lymphocystivirus*, and *Megalocytivirus* (8). Infectious spleen and kidney necrosis virus (ISKNV) is the type species of the genus *Megalocytivirus*. ISKNV was first isolated from mandarin fish (*Siniperca chuatsi*) in 1998 (23). It has been implicated in infections of more than 50 fish species and currently threatens the aquaculture industry, causing great economic losses in China (19). Within the last 3 decades, the mechanism of cellular entry of iridoviruses has been considered to be receptor-mediated clathrin endocytosis, based on the observation of the entry of frog virus 3 (FV3), the type species of the genus *Ranavirus*, into mammalian cells (BHK-21) at 28°C. In the early 1980s, transmission electron micrographic observations of FV3 entry revealed that enveloped FV3 particles were internalized by adsorptive endocytosis via coated pits and then moved through endosomes and, finally, lysosomes (5). Thus far, studies of the mechanisms of FV3 entry, replication, assembly, and budding are recognized as the model for the iridovirus life cycle (8). Recently, research on the uptake of tiger frog virus (TFV) (a ranavirus) into mammalian cells (HepG2) at 27°C showed that it is a pH-dependent atypical caveola-dependent endocytosis (21). In addition, mandarin fish caveolin-1 may play a key role in ISKNV infection, as identified previously by our laboratory (22). These differences in endocytosis pathways taken by viruses from the same genus may be caused by their infection of different hosts (9). An increasing number of fish iridoviruses have been isolated, and many viral structure genes and nonstructural genes have been identified (8). However, little is yet known about the early events of fish iridovirus infection and their mechanisms of cellular entry into their host cells.

In this study, we use pharmaceutical and molecular methods to investigate the main internalization mechanism of ISKNV entry into mandarin fish fry (MFF-1) cells. Our data show that ISKNV enters MFF-1 cells via caveolae, which is pH independent and cholesterol and dynamin dependent.

MATERIALS AND METHODS

Cells and virus. Mandarin fish fry (MFF-1) cells were maintained in Dulbecco's modified Eagle's medium (DMEM) supplemented with 10% fetal bovine serum (FBS) at 27°C under a humidified atmosphere containing 5% CO_2. An ISKNV strain adapted to grow in MFF-1 cells was used in all experiments. ISKNV cell-free virus was prepared as previously reported (13), and the titer was determined by a plaque assay.

Antibodies and reagents. Mouse polyclonal serum antibodies against mandarin fish caveolin-1 (anti-mCav-1) antibody and rabbit polyclonal serum antibodies against the ISKNV structural protein ORF101L (anti-ORF101L) were prepared as previously reported (14, 22). Rabbit anti-β-tubulin monoclonal antibodies were purchased from Epitomics, Inc. (Burlingame, CA). Goat anti-mouse IgG and goat anti-rabbit IgG conjugated with alkaline phosphatase were purchased from Promega (Madison, WI). Alexa Fluor 488-labeled goat anti-mouse IgG, Alexa Fluor 555-labeled goat anti-rabbit IgG, Alexa Fluor 488-labeled low-density lipoprotein (LDL) (AF488-LDL), and Hoechst 33342 were obtained from Invitrogen Corporation (Carlsbad, CA). The chemicals used in this study were purchased from Sigma-Aldrich (St. Louis, MO). Most chemicals were diluted in dimethyl sulfoxide (DMSO) solution according to the manufacturer's instructions, including filipin III, wortmannin, genistein, methyl-β-cyclodextrin (MβCD), nystatin, progesterone, phorbol 12-myristate 13-acetate (PMA), cholesterol, dynasore, and nocodazole, while the chemicals ammonium chloride (NH_4Cl), sucrose, chloroquine (CQ), and chlorpromazine (CPZ) were diluted in distilled water.

Infection kinetics of ISKNV. MFF-1 cells were seeded onto coverslips in 48-well plates and then exposed to ISKNV at a multiplicity of infection (MOI) of 10 and incubated at 27°C for 0, 1, 2, 3, 4, 5, 6, 7, 8, 12, 16, and 24 h. Noninternalized viruses were inactivated by using citrate buffer (40 mM sodium citrate, 10 mM KCl, and 135 mM NaCl at pH 3.1) for 2 to 3 min. About 72 h after infection, the cells were processed via an immunofluorescence assay (IFA) using the anti-ORF101L antibody.

Entry kinetics of ISKNV. Cells were seeded onto coverslips in 48-well plates 1 day prior to binding and prechilled at 4°C immediately before the experiment was conducted. ISKNV was diluted in medium and added to the prechilled cells. After virus was absorbed at 4°C for 1 h, the cells were washed with ice-cold phosphate-buffered saline (PBS) (137 mM NaCl, 2.7 mM KCl, 100 mM Na_2HPO_4, 2 mM KH_2PO_4) before fresh medium was added. The virus inocula were inactivated and removed by washing once with citrate buffer at 0, 0.5, 1, 1.5, 2, 3, 4, 5, and 6 h after a shift to 27°C. The cells were thereafter grown for 72 h in DMEM with 10% FBS and then processed for IFAs.

Drug treatments of MFF-1 cells during ISKNV infection. MFF-1 cells grown on coverslips were treated with various chemicals for 1 h prior to ISKNV infection. Control cells were incubated in medium with the corresponding solvent. The cells were then infected with ISKNV for 4 h at 27°C in the continued presence of the chemicals. After 4 h, the cells were washed once with citrate buffer to inactivate the virus and three times with PBS and then incubated with DMEM plus 10% FBS for 72 h. The cells were then fixed and analyzed by IFA. CPZ, NH_4Cl, CQ, and sucrose were used to inhibit clathrin-mediated endocytosis; filipin III, nystatin, genistein, MβCD, and PMA were used to inhibit caveola-mediated endocytosis; nocodazole was used to disrupt the microtubule structure; dynasore was used to inhibit dynamin; and wortmannin was used as a phosphoinositide 3-kinase (PI3K) inhibitor.

Western blotting. Virus internalization was analyzed by immunoblotting analysis using the anti-ORF101L antibody. Standard immunoblotting involved proteins separated by SDS-PAGE and transferred onto nitrocellulose. After 72 h of infection with ISKNV, the cells were lysed with lysis buffer containing 50 mM Tris-HCl (pH 6.8), 2% SDS, and 100 μM β-mercaptoethanol supplemented with a protease inhibitor cocktail (catalog no. 539134; Calbiochem). The protein concentrations in the cell lysates were determined by using a DC protein assay kit (Bio-Rad). Exactly 100 μg of each protein was resolved by SDS-PAGE and electrotransferred onto polyvinylidene difluoride (PVDF) membranes. After blocking with 5% nonfat milk in Tris-buffered saline (TBS)–Tween (TBST) (50 mM Tris, 150 mM NaCl, 0.05% Tween 20) for 1 h, the membranes were incubated with anti-ORF101L antibodies for 1 h at room temperature. After washing with TBST, the membrane was further incubated with goat anti-rabbit IgG conjugated with alkaline phosphatase (1:5,000 dilutions in TBST) as the secondary antibody for 1 h. The color reaction was developed by using an alkaline phosphatase chromogen (nitroblue tetrazolium

[NBT]–5-bromo-4-chloro-3-indolylphosphate [BCIP]) substrate solution. Endogenous β-tubulin (as an internal control protein) was detected by using an anti-β-tubulin antibody. The bands of Western blot (WB) results were quantified and analyzed by use of Quantity One v4.62 software, and the data were then expressed as means ± standard deviations (SDs) and analyzed by using SPSS v13.0 software.

IFA. To visualize the internalization of LDL, MFF-1 cells grown on coverslips were incubated with AF488-LDL for 30 min at 27°C. Unbound LDL was removed by washing the cells with citrate buffer. Cells grown on glass coverslips were infected with ISKNV and then treated with the drugs described above. At 72 h postinfection, the cells were washed three times with TBS and then fixed with methanol at −20°C for 5 min. At this time, the cells were washed three times with TBS, permeabilized by incubation with TBS–0.5% Triton X-100 for 15 min, and incubated with a blocking buffer (TBS containing 5% goat serum and 1% bovine serum albumin [BSA]) at 37°C for 30 min. After three washes with TBS, the coverslips were incubated with primary antibodies diluted in blocking buffer for 1 h. After that, the coverslips were rinsed four times with TBS and then incubated with the appropriate Alexa Fluor 488-labeled goat anti-mouse IgG or Alexa Fluor 555-labeled goat anti-rabbit IgG as a secondary antibody in blocking buffer for 1 h. The coverslips were stained with Hoechst 33342, followed by three washes with TBS. The cells were viewed, and micrographs were captured with a Zeiss microscope.

Cholesterol replenishment of MβCD-treated MFF-1 cells. The exchange of membrane cholesterol for exogenous cholesterol required the initial removal of cholesterol from the MFF-1 cell membrane by MβCD treatment and the subsequent replenishment of cholesterol in the depleted cells. The cells were treated with MβCD for 1 h at 27°C. This step was followed by the addition of 10, 50, or 100 μg/ml exogenous cholesterol into the medium containing MβCD, and the samples were incubated with ISKNV for 4 h at 27°C. The cells were then prepared for IFAs.

Immunofluorescence labeling and confocal microscopy. Subconfluent MFF-1 cells grown on coverslips were prechilled and then infected with ISKNV. At 1 h postinfection, the cells were rinsed with TBS and replenished with fresh DMEM. The cells were then incubated at 27°C for the indicated times and subsequently washed with TBS and fixed with methanol. The cells were analyzed by IFA using anti-mCav-1 and anti-ORF101L antibodies and then viewed under a confocal microscope (LSM510; Zeiss) equipped with 555/488-nm argon-krypton and 543-nm helium-neon lasers.

RESULTS

ISKNV infection is a slow process. Virus entry via clathrin-coated vesicles mediates the fast and efficient transfer of receptor-bound particles to an acidic endosomal compartment, whereas the internalization processes of virus endocytosis via caveolae were reported previously to be slower than the other endocytosis mechanism (2). Thus, to characterize the ISKNV entry mechanism, our initial step was to determine virus infection of and entry kinetics in MFF-1 cells. To investigate the infection kinetics of ISKNV, MFF-1 cells were infected with ISKNV, and the noninternalized viruses were removed by washing the cells with citrate buffer at the different times indicated. As shown in Fig. 1A, only about 6% of MFF-1 cells were infected after 1 h of exposure to ISKNV. Furthermore, the time of infection reached the half-maximal infection level ($t_{1/2}$) about 7 h after the addition of virus.

To determine the process of internalization into cells, the entry kinetics were also analyzed. The cells were prechilled and then infected with ISKNV (MOI = 10) for 1 h at 4°C. Under these conditions, the virus bound to the cell surface, but internalization did not occur. After washing with cold PBS to remove unbound viruses, the cells were incubated at 27°C to allow the internalization of virus to begin. At different times, noninternalized ISKNV was inactivated with citrate buffer and then incubated at 27°C for 72 h. Infection was scored by IFA. As expected, ISKNV entered MFF-1 cells primarily between 2 and 4 h after the initiation of infection (Fig. 1B). Slow entry kinetics is one of the characteristics of caveola-dependent entry (2). These results indicated that ISKNV entry into MFF-1 cells may be a caveola-dependent and not a clathrin-dependent endocytosis pathway.

ISKNV entry and infection are clathrin independent. To investigate the early steps of ISKNV infection of MFF-1 cells, inhibitors that specifically block different entry pathways were used. Since iridovirus endocytosis was previously described to be clathrin dependent (8), different from slow ISKNV infection, the role of clathrin-dependent endocytosis was first evaluated by using several disrupting drugs.

The effect of hypertonic medium (300 mM sucrose) was first investigated, resulting in the dissociation of clathrin vesicles from the plasma membrane (34). The IFA was performed by using an anti-ORF101L antibody, and the ISKNV infection rate was then scored. As shown in Fig. 1C, treatment with 100, 150, 200, 250, and 300 mM sucrose did not inhibit ISKNV infection compared to the untreated control (0 mM). Similar results were also observed by Western blotting. Therefore, the dissociation of clathrin vesicles from plasma membranes did not significantly affect ISKNV infection.

For further confirmation, CPZ was used to inhibit clathrin. CPZ causes clathrin lattices to assemble on endosomal membranes while inducing the misassembly of clathrin-coated pits at the plasma membrane (4). As shown in Fig. 1D, in the cells treated with CPZ, virus infection was minimally inhibited at 72 h postinfection, even at the highest dose (35 μM), as seen via IFA and Western blotting.

To verify the effects of these two drugs on clathrin-mediated endocytosis, we applied AF488-LDL, which was reported previously to enter via the clathrin-mediated pathway, as a positive control (29). Cells were pretreated with or without drugs under the same conditions as those used for the ISKNV infection assay, followed by incubation with AF488-LDL for 30 min in the presence or absence of the corresponding drugs. Uninternalized LDL was washed away by washing cells with citrate buffer. Figure 1E shows that both sucrose and CPZ completely blocked the internalization of AF488-LDL compared to mock-treated cells, which demonstrates the specific disruption of clathrin-mediated endocytosis by these two drugs (Fig. 1C and D). All the results indicated that the entry of ISKNV into MFF-1 cells was independent of clathrin.

Entry of ISKNV is dependent on membrane cholesterol. Next, we evaluated whether or not ISKNV internalization occurs via caveola-mediated endocytosis. Caveolae are formed from lipid rafts, consisting of cholesterol and sphingolipids, in the exoplasmic leaflet; i.e., cholesterol is a prominent compound of lipid rafts, which are involved in caveola formation, and the depletion of this compound from the membranes with MβCD impairs caveola-mediated endocytosis (46). Thus, to clearly define the role of membrane cholesterol in viral entry, the effect of MβCD on ISKNV entry into MFF-1 cells was studied. As shown in Fig. 2A (left), treatment of the cells with 1, 1.5, and 1.8 mM MβCD inhibited ISKNV infection by 45%, 60%, and 70%, respectively, compared to the untreated control (0 mM), whereas no significant inhibition was observed with 0.5 mM MβCD. Western blotting results also showed an inhibitory effect of MβCD on the expres-

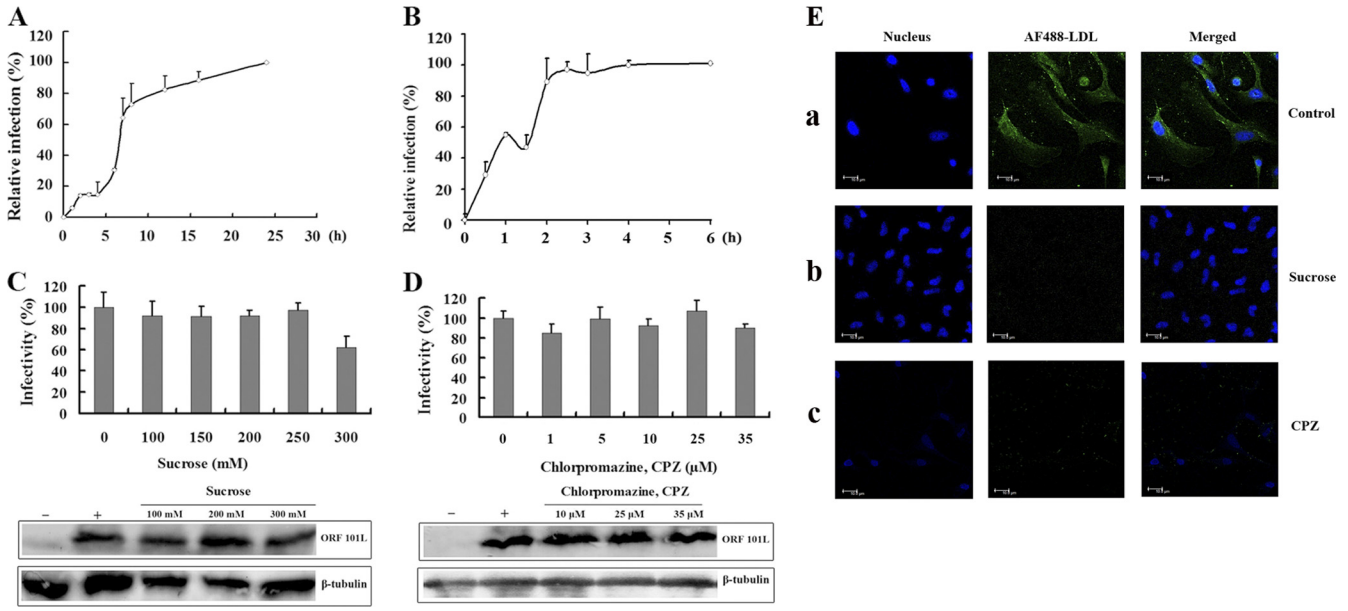

FIG 1 ISKNV infection with MFF-1 cells is a slow process and is independent of endocytosis via clathrin. (A) Infection kinetics of ISKNV. MFF-1 cells were exposed to ISKNV, and at the indicated time points, noninternalized viruses were inactivated by using citrate buffer (pH 3.1). At 72 h postinfection, the cells were detected by an immunofluorescence assay (IFA) using the anti-ORF101L antibody, and the infected cells were then counted. The values for viral infectivity are normalized to the 24-h value. The data shown represent the arithmetic means and standard deviations from three independent experiments. (B) Entry kinetics of ISKNV. ISKNV was bound to MFF-1 cells at 4°C, and the cells were washed to remove the unbound viruses. At the indicated time points, noninternalized viruses were inactivated by using citrate buffer. At 72 h postinfection, positive cells were detected by IFA and then counted. The values of viral infectivity are normalized to the 4-h value. (C and D) Effects of inhibitors of endocytosis via clathrin, sucrose (C) and chlorpromazine (CPZ) (D), on ISKNV infection. The cells were pretreated for 1 h with various concentrations of the reagents as indicated or were not treated (as a positive control), and ISKNV was then added and incubated for 4 h. After 72 h of incubation, cells were processed for IFA or Western blotting with anti-ORF101L antibody. For IFA, viral infections were quantified as the percentage of positive, treated cells relative to the number of untreated control cells. The viral infection rate of cells not treated with reagents (as a positive control) was arbitrarily set as 100%. The data shown are the means and standard deviations of the results from three independent experiments. For Western blotting, endogenous β-tubulin was included as an internal loading control. Lanes marked "+" indicate untreated control cells, and lanes marked "−" indicate the negative controls without ISKNV infection. (E) Effects of CPZ and sucrose on AF488-LDL entry into MFF-1 cells. Cells were pretreated with sucrose (200 mM) (b) or CPZ (10 μM) (c) for 1 h at 27°C and then incubated with AF488-LDL for 30 min at 27°C in the continued presence of the drugs. Panels a indicate control cells without drug treatment but with AF488-LDL incubation.

sion of the ISKNV structural protein ORF101L. As shown in Fig. 2A (right), 0.5 mM MβCD did not significantly change the level of the ORF101L protein; however, ORF101L expression was significantly inhibited by 1.8 mM MβCD. In contrast, under the same conditions as those used to block ISKNV internalization, MβCD seemed to have no effect on the internalization of LDL (Fig. 2E). These results suggest that the depletion of cellular cholesterol resulted in a significant reduction of subsequent ISKNV infection.

If the effects of MβCD on ISKNV infection were due to the removal of cholesterol, the replenishment of cholesterol after MβCD treatment should restore infection. After treatment with 1.8 mM MβCD for 1 h, the cells were allowed to recover either in cholesterol-free medium or in cholesterol-supplemented medium, which resulted in a nearly complete restoration of infection levels. As shown in Fig. 2B, ISKNV infection was significantly inhibited in cells treated with 1.8 mM MβCD alone, and the rate of infection was only ~30%. With the replenishment of the cells with 10 to 100 μg/ml cholesterol, the ISKNV infection rate increased from ~30% to ~80%. The cholesterol replenishment resulted in a dose-dependent reversal of the inhibitory effect of MβCD on ISKNV infection; i.e., cholesterol depletion is likely to be responsible for the observed inhibition.

The acute effect of cholesterol depletion by MβCD may also result in the inhibition of cholesterol-independent endocytosis (25). To exclude this possibility, the combination of the cholesterol-binding drug nystatin or filipin III and the cholesterol synthesis inhibitor progesterone was studied. Caveolae are highly enriched with cholesterol, the invagination of which requires certain conditions formed by cholesterol and caveolin-1. Consequently, sequestration with the sterol-binding drugs filipin III and nystatin will diminish the internalization of ISKNV entry via caveola-dependent endocytosis. As shown in Fig. 2C, at the highest concentration of nystatin (100 μg/ml) or filipin III (50 μg/ml) along with 20 μg/ml progesterone, ISKNV infection was reduced by around 50% compared to virus infection of control cells. As determined by Western blotting, the expression of ORF101L in ISKNV-infected cells was significantly inhibited by 100 μg/ml nystatin or 50 μg/ml filipin III with 20 μg/ml progesterone (Fig. 2D).

These results verify the role of cholesterol in the internalization of ISKNV into MFF-1 cells and suggest that ISKNV enters MFF-1 cells through the caveola-dependent endocytosis pathway.

ISKNV entry into MFF-1 cells is caveola dependent. Endocytosis via caveolae is clathrin independent, sensitive to cholesterol depletion, associated with signaling events, and dynamin dependent. Since caveolar budding is regulated by reversible phosphorylation (36), the effects of PMA, genistein, and wortmannin on ISKNV infection were determined. Activators of protein kinase C,

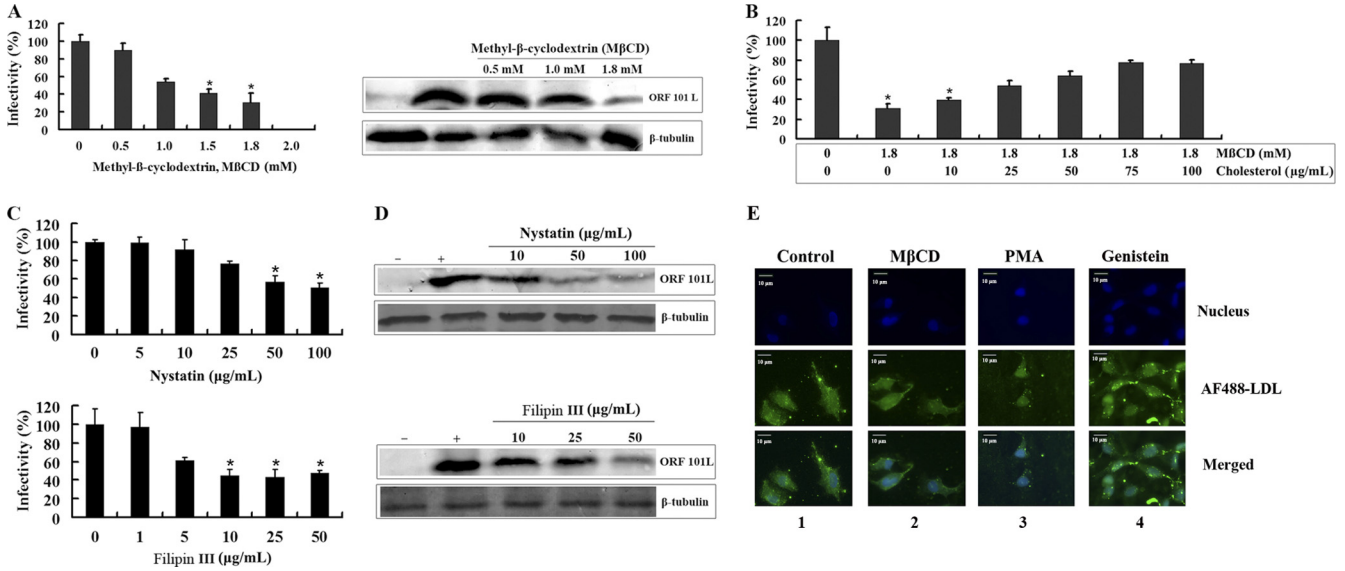

FIG 2 Effects of methyl-β-cyclodextrin (MβCD), nystatin, and filipin III on ISKNV infection. (A) MβCD inhibits ISKNV infection. Cells were pretreated for 1 h with various concentrations of reagents as indicated or were left untreated (as a positive control), and ISKNV was then added and incubated for 4 h. After 72 h of incubation, cells were processed for IFA or WB with anti-ORF101L antibody. (B) Cholesterol replenishment of MβCD-treated cells infected with ISKNV. Cells were pretreated with MβCD as described above. This step was followed by the addition of various concentrations of exogenous cholesterol as indicated, and ISKNV was then added and incubated for 4 h. (C and D) Effects of nystatin and filipin III on ISKNV infection detected by IFA (C) and WB (D). Cells were pretreated for 1 h with various concentrations of reagents as indicated along with 20 μg/ml progesterone or were left untreated (as a positive control), and ISKNV was then added and incubated for 4 h. After 72 h of incubation, the above-described samples were processed for IFA or WB with anti-ORF101L antibody. For IFA, viral infections were quantified as the percentage of positive, treated cells relative to the number of untreated control cells. The viral infection rate of cells not treated with reagents (as a positive control) was arbitrarily set as 100%. The data shown are the means and standard deviations of the results from three independent experiments. *, $P < 0.05$. For WB, endogenous β-tubulin was included as an internal loading control. Lanes marked "+" indicate untreated control cells, and lanes marked "−" indicate the negative controls without ISKNV infection. (E) Effects of specific caveola-dependent pathway inhibitors on the uptake of AF488-LDL. MFF-1 cells were pretreated with MβCD (1.8 mM) (lane 2), PMA (10 μM) (lane 3), or genistein (50 μM) (lane 3) for 1 h at 27°C and then incubated with AFF488-LDL for 30 min at 27°C in the continued presence of the drugs. Lanes 1 indicate control cells incubated with AFF488-LDL without any drug treatments.

such as the phorbol ester PMA, disrupt caveolae and block their invagination (1). As shown in Fig. 3A, the effect of the treatment of MFF-1 cells with different doses of PMA (0.1, 0.5, 1, 5, and 10 μM) was a dose-dependent reduction of ISKNV infection. At 10 μM, the rate of infection by ISKNV decreased to less than 20% compared to the infection of control cells. The expression levels of ORF101L were also significantly inhibited by 10 μM PMA, as shown by Western blotting.

Previous research on JCV and SV40 showed that signal induction is important for viral entry; therefore, we examined whether or not ISKNV also induced a signal essential for its entry. Genistein, a tyrosine kinase inhibitor, blocks the signals induced by JCV and SV40 (45), so we determined whether or not this chemical was also capable of blocking the entry of ISKNV. This part of the experiment was performed by using the assay described above; the infection rate was determined by IFA at 72 h post-ISKNV infection. As shown in Fig. 3B, the infectious entry of ISKNV was completely inhibited with 50 μM genistein; the expression of ORF101L was significantly inhibited with 25 μM genistein and nearly completely blocked with 50 μM genistein. To establish a control for the possible effects of PMA and genistein on clathrin-mediated endocytosis, we measured the effects of these drugs on the internalization of AF488-LDL under the same conditions as those used to block SV40 internalization. No significant inhibitions of the internalization of LDL into MFF-1 cells were seen in our experiments (Fig. 2E). These results indicate that ISKNV-induced transmembrane signaling is important for efficient viral entry into host cells.

Recently, several kinds of receptors were found abundantly in caveolae, including the inhibitory regulative G protein (Gi)-coupled receptor. It was reported that the activation of the Gi-coupled Src kinase pathway plays an important role in the formation and migration of endocytosis vesicles in the caveola-mediated pathway (15, 35), and the PI3K inhibitor wortmannin inhibited Gi-coupled receptor-stimulated Ras activation. Thus, the effect of wortmannin on infection by ISKNV is worth studying. Our results showed an approximately 50% inhibition of ISKNV infection; wortmannin also inhibited the expression of ORF101L (Fig. 3C). Gi signaling plays an important role in the internalization of ISKNV into MFF-1 cells.

These results suggest that ISKNV internalization into MFF-1 cells may involve signaling events associated with Src kinases and further verify that ISKNV entry into MFF-1 cells requires caveola-dependent endocytosis.

ISKNV entry into MFF-1 cells involves pH-independent endocytosis. Virus entry via clathrin-mediated endocytosis is sensitive to changes in pH. pH-dependent atypical caveola-mediated endocytosis through the *trans*-Golgi network (pH 6.0 to 6.7) was found for the entry of BK virus into permissive Vero cells and for the entry of tiger frog virus into HepG2 cells, while the classical caveola-dependent endocytosis pathway is pH independent (16, 21). To determine whether or not ISKNV entry into MFF-1 cells is

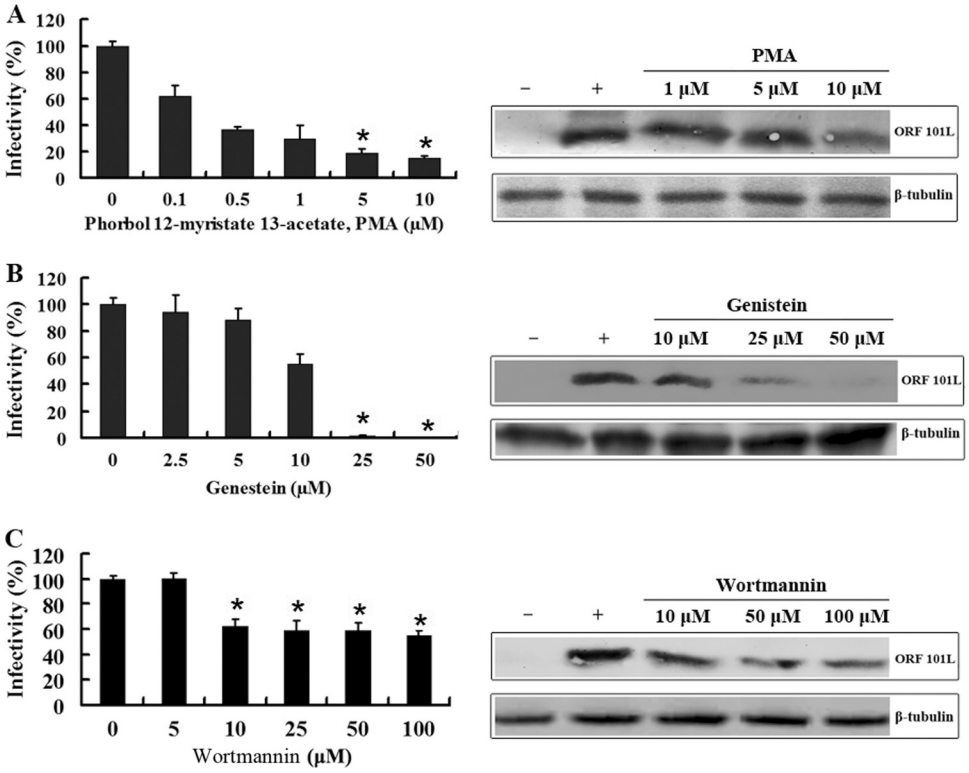

FIG 3 Effects of the inhibitors PMA (A), genistein (B), and wortmannin (C) on ISKNV infection. The cells were pretreated for 1 h with various concentrations of the reagents as indicated or were left untreated (as a positive control), and ISKNV was then added and incubated for 4 h. After 72 h of incubation, cells were processed for IFA or WB with anti-ORF101L antibody. For IFA, viral infections were quantified as the percentage of positive, treated cells relative to the number of untreated control cells. The viral infection rate of cells not treated with reagents (as a positive control) was arbitrarily set as 100%. The data shown are the means and standard deviations of the results from three independent experiments. *, $P < 0.05$. For WB, endogenous β-tubulin was included as an internal loading control. Lanes marked "+" indicate untreated control cells, and lanes marked "−" indicate the negative controls without ISKNV infection.

independent of pH, lysosomotropic agents were used to disrupt the acidification of intracellular organelles, to determine the role of low pH in ISKNV infection. CQ and NH_4Cl are weakly basic amines that, in their neutral forms, selectively enter cellular compartments with a low internal pH and there become protonated, elevating the pH of the target organelle (13). Infections were scored by measuring the expression of the structural protein ORF101L using immunofluorescence staining. As expected (Fig. 4A), NH_4Cl and CQ treatments did not significantly inhibit ISKNV infection, even at the highest doses used (50 mM and 75 μM, respectively), compared to the untreated controls. MFF-1 cells, whether left untreated or treated with NH_4Cl or CQ, were equally susceptible to ISKNV entry. As shown by Western blotting for ORF101L expression, ISKNV-infected cells were also not significantly inhibited when cells were treated with NH_4Cl. Endogenous β-tubulin levels, included as an internal loading control for the Western blot analysis, were unaffected by the NH_4Cl treatments. Similar results were also observed for cells treated with CQ (Fig. 4B). Meanwhile, when the same treatment (50 mM NH_4Cl or 50 μM CQ) was applied to MFF-1 cells, the level of internalization of LDL dramatically decreased (Fig. 4C). These observations suggest that ISKNV entry is pH independent; i.e., ISKNV entry does not occur through atypical caveola-dependent endocytosis, further verifying that it is independent of clathrin-coated pits.

ISKNV entry and early infection events are dynamin and microtubule dependent. Dynamin is a large GTPase that forms a dynamin ring at the stem connecting the nascent vesicle to the plasma membrane and works as a motor protein involved in pinching off vesicles from the cell surface (38). Dynamin was initially considered specific to the clathrin-dependent pathway; later, however, it was found to play an important role in the initial steps of both clathrin-mediated endocytosis and caveola-mediated endocytosis (47). Its involvement in viral entry is due to the formation of nascent coated vesicles, e.g., clathrin- or caveolin-coated vesicles, at the plasma membrane. These coated vesicles form and pinch off by a controlled mechanism that involves several proteins, including dynamin. Dynasore, a dynamin inhibitor that prevents the scission of dynamin-dependent endocytosis vesicles, is a cell-permeable semicarbazone compound that inhibits the GTPase activity of dynamin-1 and dynamin-2 (32). Dynasore has been used to elucidate the roles of dynamin-dependent endocytosis, both clathrin dependent and caveola dependent (18). In this study, we tested whether or not ISKNV infection can be blocked by dynasore. As shown in Fig. 5A, the infectious entry of ISKNV was 55% to 65% inhibited by 25 to 50 μM dynasore in the IFA, and ORF101L expression was significantly inhibited by 50 μM dynasore in the Western blot analysis. These results demonstrate that dynasore blocks ISKNV infection of MFF-1 cells in a dose-dependent manner and that ISKNV entry into MFF-1 cells is dynamin dependent via the caveola-mediated endocytosis pathway.

Research regarding caveola-dependent endocytosis revealed that the classical caveola-mediated endocytosis pathway is depen-

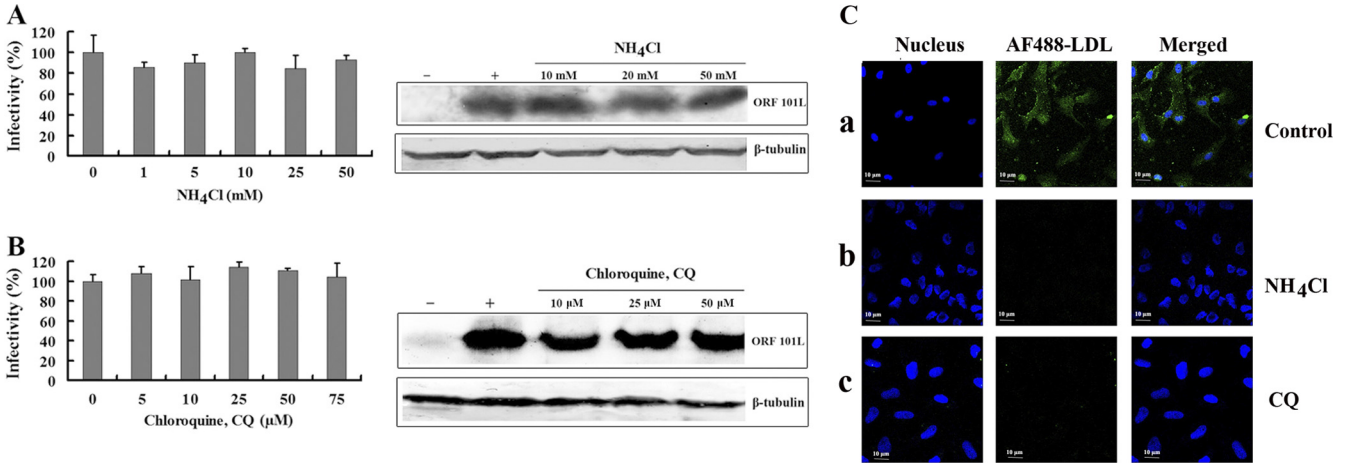

FIG 4 (A and B) Effects of NH_4Cl (A) and chloroquine (CQ) (B) on ISKNV infection. Cells were pretreated for 1 h with various concentrations of reagents as indicated or were left untreated (as a positive control), and ISKNV was then added and incubated for 4 h. After 72 h of incubation, the cells were processed for IFA or WB with anti-ORF101L antibody. For the IFA, the viral infections were quantified as the percentage of positive, treated cells relative to the number of untreated control cells. The viral infection rate of cells not treated with reagents (as a positive control) was arbitrarily set as 100%. The data shown are the means and standard deviations of the results from three independent experiments. For WB, endogenous β-tubulin was included as an internal loading control. Lanes marked "+" indicate untreated control cells, and lanes marked "−" indicate the negative controls without ISKNV infection. (C) Internalization of AF488-LDL into MFF-1 cells treated with lysosomotropic agents. Cells were mock treated (no drugs) (a) or pretreated with NH_4Cl (50 mM) (b) or CQ (50 μM) (c), followed by incubation with AF488-LDL for 30 min.

dent on microtubules that serve as tracks along which motile cavicles move via a caveola-caveosome-ER pathway, such as in SV40 (41), while the uptake of AMF is independent of microtubules, and AMF is delivered directly from caveolae to the Golgi complex-ER (31). To determine whether or not microtubules are involved in ISKNV entry, nocodazole, a microtubule-dissociating drug, was used. As shown in Fig. 5B, the treatment of cells with 10 μM nocodazole dramatically decreased (about an 80% reduction) ISKNV infection compared to the untreated controls. Western blotting showed that treatment with 1 to 10 μM nocodazole did not result in a significant reduction of the levels of tubulin, but the expression levels of ORF101L were also significantly inhibited by >5 μM nocodazole. These results suggest that ISKNV entry into MFF-1 cells is dependent on microtubules and proceeds via the caveosome pathway.

Use of confocal microscopy to determine the locations of caveolin-1 and ISKNV. To further confirm that ISKNV enters MFF-1 cells via the caveola endocytosis pathway, immunofluores-

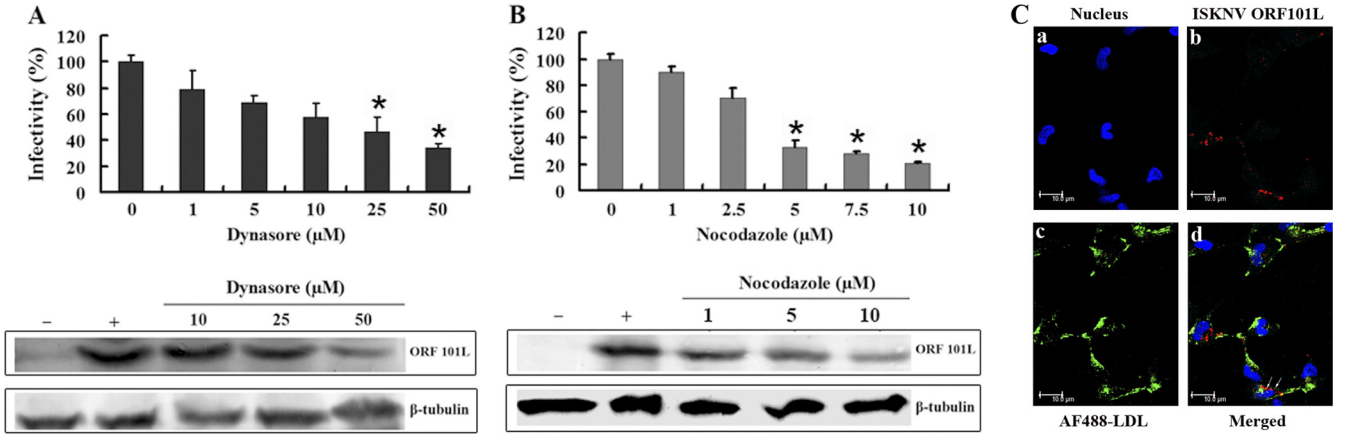

FIG 5 Effects of dynasore and nocodazole on ISKNV infection. (A and B) Cells were pretreated for 1 h with dynasore (A) or nocodazole (B) with various concentrations of reagents as indicated or were left untreated (as a positive control), and ISKNV was then added and incubated for 4 h. After 72 h of incubation, the cells were processed for IFA or WB with anti-ORF101L antibody. For IFA, viral infections were quantified as the percentage of positive, treated cells relative to the number of untreated control cells. The viral infection rate of cells not treated with reagents (as a positive control) was arbitrarily set as 100%. The data shown are the means and standard deviations of the results from three independent experiments. *, $P < 0.05$. For WB, endogenous β-tubulin was included as an internal loading control. Lanes marked "+" indicate untreated control cells, and lanes marked "−" indicate the negative controls without ISKNV infection. (C) Internalization of AF488-LDL and ISKNV into MFF-1 cells. Cells grown on coverslips were prechilled and then infected with ISKNV at 4°C for 1 h, and noninternalized viruses were then washed by using TBS, while the uninfected cells were used as a negative control. Cells were incubated with 50 μg of AF488-LDL for 30 min at 4°C for binding, washed, transferred to 27°C for 30 min, and then fixed with methanol. The cells were analyzed by IFA using anti-ORF101L antibodies and were then viewed under a confocal microscope (LSM510; Zeiss). ISKNV particles (red fluorescence), AF488-LDL (green fluorescence), and nuclei (blue fluorescence) were visualized with Hoechst 33342.

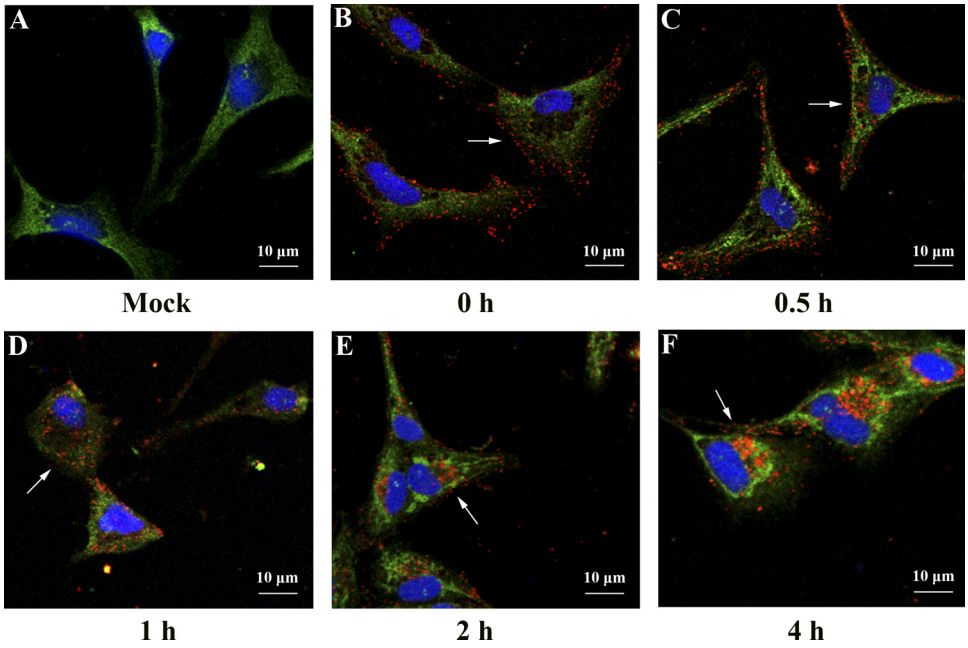

FIG 6 Confocal microscopy of ISKNV internalization into MFF-1 cells. Cells grown on coverslips were prechilled and then infected with ISKNV at 4°C for 1 h. Noninternalized viruses were washed up by using TBS and fixed with methanol at 0 h (B), 0.5 h (C), 1 h (D), 2 h (E), and 4 h (F), while uninfected cells (A) were used as a negative control. The cells were analyzed by IFA using anti-mCav-1 and anti-ORF101L antibodies and were then viewed under a confocal microscope (LSM510; Zeiss) equipped with 555/488-nm argon-krypton and 543-nm helium-neon lasers. ISKNV particles (red fluorescence), mandarin fish caveolin-1 (green fluorescence), and nuclei (blue fluorescence) were visualized with Hoechst 33342. Magnification, ×600.

cence labeling of ISKNV was performed by labeling with an anti-ORF101L antibody and the caveola marker caveolin-1. Double labeling with anti-ORF101L and anti-mCav-1 antibodies at different times showed colocalization. As shown in Fig. 6, no colocalization was seen at 0 h (Fig. 6B, arrow), indicating that although ISKNVs are bound to the membrane, they did not appear at the caveola domain; at 0.5 to 1 h, colocalization increased with the internalization of ISKNVs (Fig. 6C and D, arrowed), and at 2 h postinfection, significant colocalization was seen (Fig. 6E, arrows). At 4 h postinfection, ISKNV approached the nucleus (Fig. 6F, arrow). Taking into consideration the results described above and in our previous study on the location of caveolin-1 in MFF-1 cells, the ubiquitous location of caveolin-1 makes this colocation not so persuasive. To reinforce our conclusion, we performed a confocal experiment with ISKNV and AF488-LDL. No colocalization was observed with this assay (Fig. 5C), thus indicating that the two employed different ways of entering MFF-1 cells.

DISCUSSION

Viruses that enter cells by endocytosis generally penetrate via different pathways, two of which are the most frequently used: the clathrin-mediated pathway and the caveola-mediated endocytosis pathway. In this study, inhibitors that specifically block different entry pathways were used to investigate the early steps of ISKNV infection of MFF-1 cells. Therefore, cell viability and toxicological tests with most inhibitors were performed as previously described, using Cell Counting Kit 8 (CCK-8) (21). The inhibitors, at the concentrations used in this study, did not exhibit cytotoxic activity against MFF-1 cells (data not shown).

Endocytosis through clathrin-coated vesicles is pH sensitive and clathrin dependent. In SFV and vesicular stomatitis virus (VSV), which are endocytosed via CCPs, this process is very rapid (28). AF488-LDL, a ligand endocytosed by the clathrin-mediated pathway (CMP), also exhibits this rapid process: it took only 30 min for AF488-LDL to enter MFF-1 cells under our experimental conditions. In contrast, ISKNV is internalized remarkably slowly. ISKNV infection of MFF-1 cells reached the half-maximal infection level ($t_{1/2}$) about 7 h after the addition of virus, whereas VSV reaches the $t_{1/2}$ after just 1.5 h (47). Slow infection kinetics were also observed previously for the entry of amphotropic murine leukemia virus into NIH 3T3 cells by caveola-dependent endocytosis, reaching the $t_{1/2}$ at about 5 h postinfection (2). The entry kinetics confirmed that ISKNV enters MFF-1 cells with delayed kinetics; ISKNV (~50 min) needed almost 3 to 4 times longer to enter cells and to reach the $t_{1/2}$ did than VSV or SFV (10 to 20 min), consistent with data from previous studies on virus entry via caveolae (2). Furthermore, the inhibitors of the dissociation of clathrin vesicles from the plasma membrane (CPZ and sucrose) and cytosol acidification chemicals (NH_4Cl and CQ) did not impair ISKNV infection. Therefore, ISKNV is internalized by a clathrin-independent pathway.

Since ISKNV infection was a slow clathrin-independent process, more similar to caveola-mediated entry, several drugs that block caveola-dependent endocytosis were used to identify the ISKNV entry points that lead to infection. Pharmacological evidence suggests that ISKNV infection is cholesterol dependent. Moreover, previous studies have shown that the internalization of caveolae is inhibited by kinase inhibitors. For example, SV40 binding to the cell surface activates a tyrosine kinase-based signaling cascade, disrupting the local actin cytoskeleton and recruiting dynamin II to caveola sites with abundant caveolin-1, and albumin binding to its receptor, gp60, triggers caveola endocytosis via

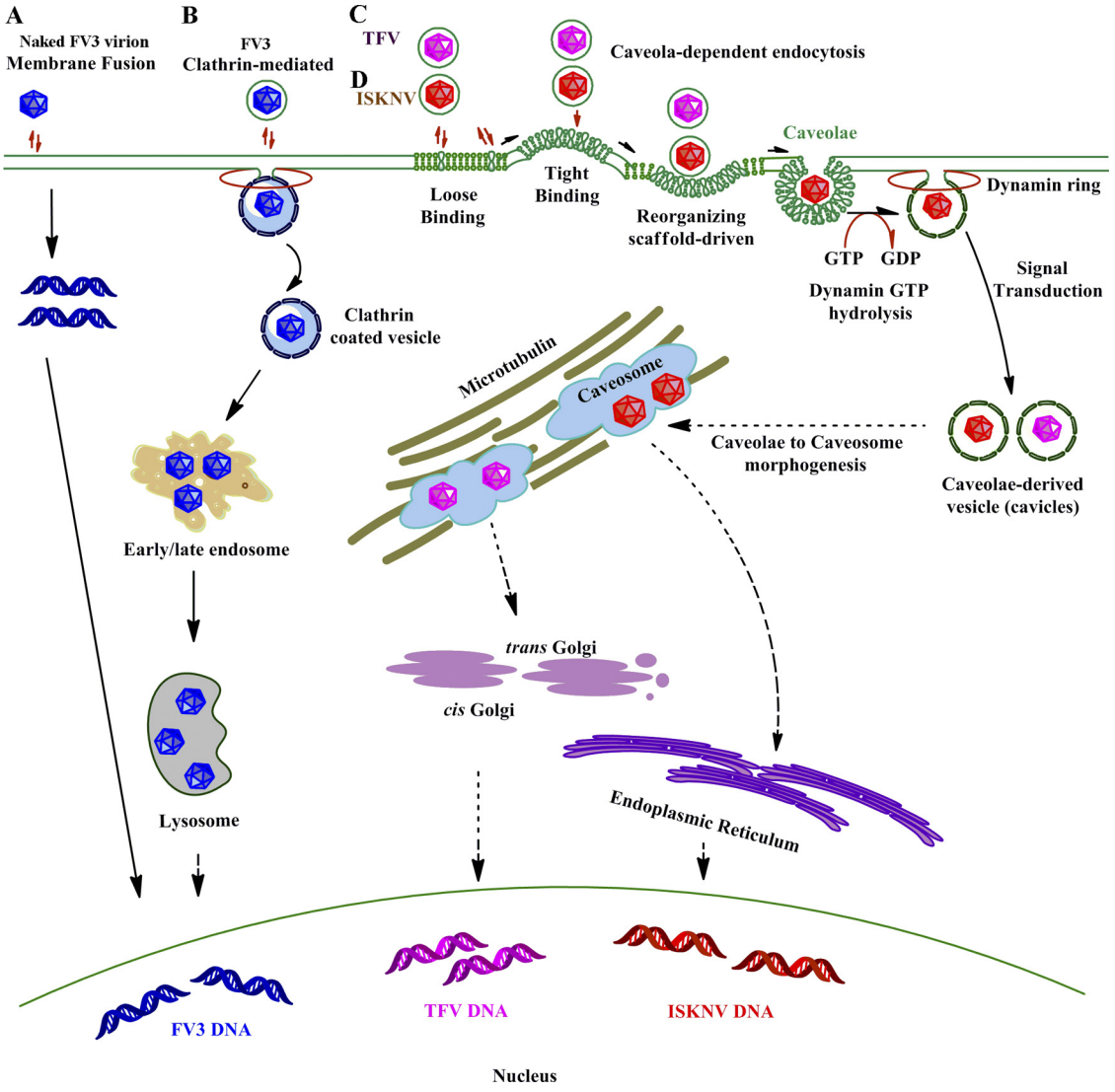

FIG 7 Models of cellular entry of iridoviruses. (A) Naked frog virus 3 (FV3) enters BHK-21 cells via membrane fusion. (B) Enveloped FV3 particles enter BHK-21 cells via clathrin-dependent endocytosis. Viruses internalize into BHK-21 cells by adsorptive endocytosis via coated pits and then appear to move through endosomes and, ultimately, to lysosomes. (C and D) Tiger frog virus (TFV) (C) and infectious spleen and kidney necrosis virus (ISKNV) (D) internalize into their host cells via caveolae.

a Gi-coupled Src kinase-mediated pathway (35). Above all, the internalization of some caveolar ligands is therefore a signal-mediated process that requires caveolin-1 expression. Our studies also prove that ISKNV infection can be inhibited by tyrosine kinase inhibitors as well as the PI3K inhibitor (Fig. 3). These results are consistent with the studies mentioned above. Caveolin-1 plays an important role in caveola formation; in a previous study, it was reported that the recombinant expression of caveolin-1 in cells devoid of caveolae led to the formation of caveola-like vesicles (49). The membrane-spanning caveolin-1 scaffolding domain (CSD), essential for membrane attachment for caveolae, has a docking role for certain signaling molecules, such as endothelial nitric oxide synthase and protein kinase A (9, 11). The caveolin-1 scaffolding domain peptide (SDP) sequence offers opportunities for direct interactions of the CSD with membranes. MFF-1 cells treated with mandarin fish SDP (mSDP) show a dramatic reduction in ISKNV infection, as previously reported (22). These observations indicate that caveolin-1 plays an important role in the formation and stabilization of caveolae and thus influences ISKNV infection. Therefore, ISKNV enters MFF-1 cells via the caveola-mediated pathway.

In addition, dynamin, a large GTPase reported to be essential for clathrin-coated vesicle formation and transportation, also plays an important role in ligand uptake through caveola-mediated endocytosis and is required for the uptake of several viruses (47). It appears to form a structural collar around the neck of caveolae that hydrolyzes GTP to mediate internalization via the fission of caveolae from the plasma membrane to form free transport vesicles (38); that is, with dynasore, which rapidly inhibits the GTPase activity of dynamin-1 and dynamin-2 with high specificity and which prevents the scission of dynamin-dependent endocytosis vesicles (32), we were able to determine whether dynamin is involved in ISKNV entry. Our results (Fig. 5A) showed that ISKNV entry was dependent on dynamin.

We then determined a model of caveola-dependent endocytosis used by ISKNV to enter MFF-1 cells. Studies of two caveolar ligands, CTx and AMF, suggest that there are two sorting methods in caveola-dependent endocytosis. CTx is delivered to a caveolin-1-positive endocytosis compartment, or caveosome, and then transported to either the Golgi complex or the ER (41). AMF, however, is delivered directly to the ER (28). These sorting methods lead to different pharmacological results. The former one can be disrupted by the microtubule-depolymerizing agent nocodazole or a 20°C temperature shift, while the latter one cannot (35). According to our results, treatment of MFF-1 cells with nocodazole could significantly impair ISKNV infection. Therefore, ISKNV may exploit the same pathway as CTx and is delivered to caveosomes.

As previously reported, three models have been proposed for the capture of caveolae/raft-clustering virus particles in membrane invaginations (40, 42). In the first model, the cholesterol concentration increases with the clustering of rafts on the membrane and results in a spontaneous curvature of the membrane. The shape of virus particles may aid the specific inward curvature. As an extension, another model was proposed. Caveolin-1 binds to cholesterol at a 1:1 ratio and cross links to glycosphingolipid. Here, caveolin-1 works as an integral, nonspanning membrane protein cotranslationally inserted from the cytosol into the membrane of the ER and forms oligomers (42). Virus-induced lipid rafts clustered on the membrane and subsequently increased the concentration of membrane-integrated scaffolding molecules, which then oligomerize on the cytosolic side. The scaffold molecules could also be recruited (42). The third model, supported by increasing evidence, suggest that 144 molecules of caveolin-1 form polymers at the Golgi complex; these polymers stay intact and are then transported to membrane sites to form a preexisting domain (42). Virus particles initially bind randomly on the membrane and are subsequently trapped and bound tightly in the preexisting caveolin-1 domains with increasing affinity. Virus particle binding may activate changes in the scaffold that promote a curved configuration. Our colocalization experiment showed that ISKNV bound to the membrane of MFF-1 cells without significant colocalization with caveolin-1, and with time, an increased colocalization of ISKNV with caveolin-1 was shown, both of which started to internalize in the MFF-1 cells and were transported to the nucleus; hence, the internalization of ISKNV fit the third model.

In summary, the data presented in this study suggest that ISKNV internalization during productive infection occurs through a caveolar mechanism. Moreover, this internalization is consistent with the third proposed model of membrane invagination. Finally, the disruption with the microtubule-depolymerizing agent nocodazole indicates that the sorting routine is similar to that of SV40, which needs the formation of compartments-caveosomes.

In the present study, ISKNV entry into fish cells through a classical caveola-dependent endocytosis pathway is first identified. The process (Fig. 7) is different from the clathrin-mediated endocytosis of FV3 into BHK-21 cells and the pH-dependent atypical caveola-mediated endocytosis of TFV into HepG2 cells (5, 21). These differences in hosts may result in this variety of endocytosis pathways taken by viruses from the same genus. The research on SV40 done previously by Damm and coworkers also suggested that SV40 is inclined to take different endocytosis pathways when hosts are devoid of key factors for the caveola-mediated pathway (12), which means that viruses may be able to develop new endocytosis pathway to infect different hosts by using the existing endocytosis-related factors in different hosts. Thus, our work may help further the understanding of the initial steps of fish iridovirus infections, facilitate the recognition of the cellular entry mechanism of megalocytiviruses, and provide valuable information for the development of new and effective antiviral targets, and by comparisons with other data on entry pathways of viruses from same genus, we may find some proof to elucidate the interactions of viruses and their hosts.

ACKNOWLEDGMENTS

We thank Xiao-Peng Xiong for kindly providing the rabbit anti-ORF101L polyclonal antibody.

This work was supported by the National Natural Science Foundation of China under grant no. U0631008 and 31001123, the National Basic Research Program of China under grant no. 2006CB101802, the National High Technology Research and Development Program of China (863 Program) under grant no. 2006AA09Z445 and 2006AA100309, the Priming Scientific Research Foundation for Junior Teachers in Sun Yat-sen University, and the China Postdoctoral Science Foundation.

REFERENCES

1. **Anderson HA, Chen Y, Norkin LC.** 1996. Bound simian virus 40 translocates to caveolin-enriched membrane domains, and its entry is inhibited by drugs that selectively disrupt caveolae. Mol. Biol. Cell **7**:1825–1834.
2. **Beer C, Andersen DS, Rojek A, Pedersen L.** 2005. Caveola-dependent endocytic entry of amphotropic murine leukemia virus. J. Virol. **79**: 10776–10787.
3. **Berryman S, Clark S, Monaghan P, Jackson T.** 2005. Early events in integrin alphavbeta6-mediated cell entry of foot-and-mouth disease virus. J. Virol. **79**:8519–8534.
4. **Blanchard E, et al.** 2006. Hepatitis C virus entry depends on clathrin-mediated endocytosis. J. Virol. **80**:6964–6972.
5. **Braunwald J, Nonnenmacher H, Tripier-Darcy F.** 1985. Ultrastructural and biochemical study of frog virus 3 uptake by BHK-21 cells. J. Gen. Virol. **66**:283–293.
6. **Chen C, Zhuang X.** 2008. Epsin 1 is a cargo-specific adaptor for the clathrin-mediated endocytosis of the influenza virus. Proc. Natl. Acad. Sci. U. S. A. **105**:11790–11795.
7. **Cheng ZJ, Singh RD, Marks DL, Pagano RE.** 2006. Membrane microdomains, caveolae, and caveolar endocytosis of sphingolipids. Mol. Membr. Biol. **23**:101–110.
8. **Chinchar VG, Hyatt A, Miyazaki T, Williams T.** 2009. Family Iridoviridae: poor viral relations no longer. Curr. Top. Microbiol. Immunol. **328**: 123–170.
9. **Chinchar VG, Yu KH, Jancovich JK.** 2011. The molecular biology of frog virus 3 and other iridoviruses infecting cold-blooded vertebrates. Viruses **3**:1959–1985.
10. **Chu JJ, Ng ML.** 2004. Infectious entry of West Nile virus occurs through a clathrin-mediated endocytic pathway. J. Virol. **78**:10543–10555.
11. **Cohen AW, Hnasko R, Schubert W, Lisanti MP.** 2004. Role of caveolae and caveolins in health and disease. Physiol. Rev. **84**:1341–1379.
12. **Damm EM, et al.** 2005. Clathrin- and caveolin-1-independent endocytosis: entry of simian virus 40 into cells devoid of caveolae. J. Cell Biol. **168**:477–488.
13. **DeTulleo L, Kirchhausen T.** 1998. The clathrin endocytic pathway in viral infection. EMBO. J. **17**:4585–4593.
14. **Dong C, et al.** 2011. Global landscape of structural proteins of infectious spleen and kidney necrosis virus. **85**:2869–2877.
15. **Dudzinski DM, Michel T.** 2007. Life history of eNOS: partners and pathways. Cardiovasc. Res. **75**:247–260.
16. **Eash S, Querbes W, Atwood WJ.** 2004. Infection of Vero cells by BK virus is dependent on caveolae. J. Virol. **78**:11583–11590.
17. **Fra AM, Williamson E, Simons K, Parton RG.** 1995. De novo formation of caveolae in lymphocytes by expression of VIP21-caveolin. Proc. Natl. Acad. Sci. U. S. A. **92**:8655–8659.
18. **García Lopez MA, Aguado Martínez A, Lamaze C, Martínez-a C,**

Fischer T. 2009. Inhibition of dynamin prevents CCL2-mediated endocytosis of CCR2 and activation of ERK1/2. Cell. Signal. **21**:1748–1757.
19. **Go J, Lancaster M, Deece K, Dhungyel O, Whittington R.** 2006. The molecular epidemiology of iridovirus in Murray cod (*Maccullochella peelii peelii*) and dwarf gourami (*Colisa lalia*) from distant biogeographical regions suggests a link between trade in ornamental fish and emerging iridoviral diseases. Mol. Cell. Probes **20**:212–222.
20. **Goorha R, Granoff A.** 1979. Icosahedral cytoplasmic deoxyriboviruses, p 347–399. *In* Fraenkel-Conrat H, Wagner RR (ed), Comprehensive virology. Plenum Publishing Corp., New York, NY.
21. **Guo CJ, et al.** 2011. Tiger frog virus (an iridovirus) entry into HepG2 cells via a pH-dependent, atypical caveola-mediated endocytosis pathway. J. Virol. **85**:6416–6426.
22. **Guo CJ, et al.** 2011. Involvement of caveolin-1 in the Jak-Stat signaling pathway and infectious spleen and kidney necrosis virus infection in mandarin fish (*Siniperca chuatsi*). Mol. Immunol. **48**:992–1000.
23. **He JG, Zeng K, Weng SP, Chan SM.** 2000. Systemic disease caused by an iridovirus-like agent in cultured mandarin fish *Siniperca chuatsi* (Basillewsky), in China. J. Fish Dis. **23**:219–222.
24. **Hernaez B, Alonso C.** 2010. Dynamin- and clathrin-dependent endocytosis in African swine fever virus entry. J. Virol. **84**:2100–2109.
25. **Imelli N, Meier O, Boucke K, Hemmi S, Greber UF.** 2004. Cholesterol is required for endocytosis and endosomal escape of adenovirus type 2. J. Virol. **78**:3089–3098.
26. **Jin M, et al.** 2002. Hantaan virus enters cells by clathrin-dependent receptor-mediated endocytosis. Virology **294**:60–69.
27. **Kee SH, et al.** 2004. Effects of endocytosis inhibitory drugs on rubella virus entry into VeroE6 cells. Microbiol. Immunol. **48**:823–829.
28. **Kielian MC, Marsh M, Helenius A.** 1986. Kinetics of endosome acidification detected by mutant and wild-type Semliki Forest virus. EMBO. J. **5**:3103–3109.
29. **Lakadamyali M, Rust MJ, Zhuang X.** 2006. Ligands for clathrin-mediated endocytosis are differentially sorted into distinct populations of early endosomes. Cell **124**:997–1009.
30. **Le PU, Guay G, Altschuler Y, Nabi IR.** 2002. Caveolin-1 is a negative regulator of caveolae-mediated endocytosis to the endoplasmic reticulum. J. Biol. Chem. **277**:3371–3379.
31. **Le PU, Nabi IR.** 2003. Distinct caveolae-mediated endocytic pathways target the Golgi apparatus and the endoplasmic reticulum. J. Cell Sci. **116**:1059–1071.
32. **Macia E, et al.** 2006. Dynasore, a cell-permeable inhibitor of dynamin. Dev. Cell **10**:839–850.
33. **Marjomäki V, Pietiäinen V, Matilainen H, Upla P.** 2002. Internalization of echovirus 1 in caveolae. J. Virol. **76**:1856–1865.
34. **Martinez MG, Cordo SM, Candurra NA.** 2007. Characterization of Junin arenavirus cell entry. J. Gen. Virol. **88**:1776–1784.
35. **Nabi IR, Le PU.** 2003. Caveolae/raft-dependent endocytosis. J. Cell Biol. **161**:673–677.
36. **Nichols B.** 2003. Caveosomes and endocytosis of lipid rafts. J. Cell Sci. **116**:4707–4714.
37. **Nomura R, et al.** 2004. Human coronavirus 229E binds to CD13 in rafts and enters the cell through caveolae. J. Virol. **78**:8701–8708.
38. **Oh P, McIntosh DP, Schnitzer JE.** 1998. Dynamin at the neck of caveolae mediates their budding to form transport vesicles by GTP-driven fission from the plasma membrane of endothelium. J. Cell Biol. **141**:101–114.
39. **Pauly BS, Drubin DG.** 2007. Clathrin: an amazing multifunctional dreamcoat? Cell Host Microbe **2**:288–290.
40. **Pelkmans L, Helenius A.** 2002. Endocytosis via caveolae. Traffic **3**:311–320.
41. **Pelkmans L, Kartenbeck J, Helenius A.** 2001. Caveolar endocytosis of simian virus 40 reveals a new two-step vesicular-transport pathway to the ER. Nat. Cell Biol. **3**:473–483.
42. **Pelkmans L.** 2005. Secrets of caveolae- and lipid raft-mediated endocytosis revealed by mammalian viruses. Biochim. Biophys. Acta **1746**:295–304.
43. **Peng T, et al.** 2009. Entry of dengue virus serotype 2 into ECV304 cells depends on clathrin-dependent endocytosis, but not on caveolae-dependent endocytosis. Can. J. Microbiol. **55**:139–145.
44. **Pho MT, Ashok A, Atwood WJ.** 2000. JC virus enters human glial cells by clathrin-dependent receptor-mediated endocytosis. J. Virol. **74**:2288–2292.
45. **Querbes W, O'Hara BA, Williams G, Atwood WJ.** 2006. Invasion of host cells by JC virus identifies a novel role for caveolae in endosomal sorting of noncaveolar ligands. J. Virol. **80**:9402–9413.
46. **Sánchez-San Martín C, López T, Arias CF, López S.** 2004. Characterization of rotavirus cell entry. J. Virol. **78**:2310–2318.
47. **Skretting G, Torgersen ML, van Deurs B, Sandvig K.** 1999. Endocytic mechanisms responsible for uptake of GPI-linked diphtheria toxin receptor. J. Cell Sci. **112**:3899–3909.
48. **Smith JL, Campos SK, Ozbun MA.** 2007. Human papillomavirus type 31 uses a caveolin 1- and dynamin 2-mediated entry pathway for infection of human keratinocytes. J. Virol. **81**:9922–9931.
49. **Vogel U, Sandvig K, van Deurs B.** 1998. Expression of caveolin-1 and polarized formation of invaginated caveolae in Caco-2 and MDCK II cells. J. Cell Sci. **111**:825–832.
50. **Vonderheit A, Helenius A.** 2005. Rab7 associates with early endosomes to mediate sorting and transport of Semliki Forest virus to late endosomes. PLoS Biol. **3**:e233.
51. **Watanabe T, Watanabe S, Kawaoka Y.** 2010. Cellular networks involved in the influenza virus life cycle. Cell Host Microbe **7**:427–439.